1484

Impact of Tissue Sample Preparation Method on Myelin-Sensitive Quantitative MR Imaging and Histological Analysis

Amaya Murguia[1], Andrea Jacobson[2], Scott D. Swanson[3], Ulrich Scheven[4], Jon-Fredrik Nielsen[2,3], Jeffrey A. Fessler[1,2,3], and Navid Seraji-Bozorgzad[5]
[1]Electrical Engineering and Computer Science, University of Michigan, Ann Arbor, MI, United States, [2]Biomedical Engineering, University of Michigan, Ann Arbor, MI, United States, [3]Radiology, University of Michigan, Ann Arbor, MI, United States, [4]Mechanical Engineering, University of Michigan, Ann Arbor, MI, United States, [5]Neurology, University of Michigan, Ann Arbor, MI, United States

Synopsis

Keywords: White Matter, White Matter

Motivation: Quantitative MRI (qMRI) parameter validation with histology is often done with ex vivo fixed tissue. Freezing is another preservation method, but the effects of freezing/thawing on qMRI parameters and their correlation with histology are unknown.

Goal(s): We investigated how freezing/thawing brain tissue affects myelin-sensitive qMRI properties and histology correlation.

Approach: We scanned the same fresh/thawed and fresh/fixed samples and compared qMRI parameters with luxol fast blue (LFB) results.

Results: qMRI values correlated well with LFB across conditions. Thawed and fixed tissues exhibited modest increases in qMRI parameters compared to fresh. Histology showed that samples did not lose tissue integrity from the freezing process.

Impact: Tissue freezing is a reasonable alternative preservation method to tissue fixation for use in qMRI analysis. Brain banks that store frozen tissue could use these samples for future qMRI and histological studies.

Introduction

Quantitative MRI (qMRI) has been proposed as a marker of disease pathology and is often validated with histology in fixed tissues[1]. However, fixation can alter MR tissue properties and histological findings[2]. Tissue freezing is a post-mortem storage method that preserves the ability to conduct immunohistochemistry, but freezing samples jeopardizes tissue integrity[3,4]. Therefore, we compared several putative myelin-sensitive qMRI parameters in fresh, thawed, and fixed samples.

Experimental Methods

Sixteen fresh sheep brain ex vivo samples were scanned in a 7T Varian/Agilent scanner using multi-echo spin echo (MESE), quantitative magnetization transfer (qMT), and inversion recovery (IR) scans according to the protocol in [5]. Eight were frozen at -80°C, thawed, and scanned again[5]; the other eight were fixed in formalin, washed in normal saline solution, and scanned again[5]. All samples were eventually fixed, underwent paraffin and luxol fast blue (LFB) embeddings, and imaged with a Vectra Polaris brightfield whole-slide scanner to calculate LFB optical density (LFB OD). Additionally, seven human ex vivo brain samples with white matter (WM) pathology from the Michigan Alzheimer's Disease Research Center (MADRC) Brain Bank were thawed from -80°C and scanned[5].

Data Processing and Statistical Methods

Non-negative least squares (NNLS) regression with B_1 estimation was performed on the MESE data to generate myelin water fraction (MWF) maps[6]. Magnetization transfer ratio (MTR) maps were calculated from the MT data, and qMT fraction (qMT-F) maps were generated using the binary spin-bath model[7,8]. A bi-exponential fit was conducted on the IR data[9]. The IR EPI distorted images were unwarped and registered to the MESE data,[10] and a short T_1 fraction (short T_1-F) map was calculated as the ratio of the fast-relaxing component amplitude divided by the sum of the fast and slow-relaxing component amplitudes. Analysis was done with MATLAB and Julia. The histology and corresponding MR images were labeled with WM and gray matter (GM) regions of interest (ROIs) with Freeview (512 ROIs across 16 samples). MR surrogate measures of myelin and LFB averages were calculated in each ROI; two-group analysis of variance (ANOVA) and unpaired t-tests and Mann–Whitney U tests were performed in R to compare the thawed/fixed groups separately to the fresh group. Both tests gave the same results, so the Mann-Whitney results are reported here. Generalized linear modeling (GLM) was performed to determine correlations between parameters. For the human samples, ROIs in WM lesions were also labeled (30 ROIs across seven samples).

Results

Figure 1 shows qMRI parameter maps for two representative samples; we observe similar contrasts across tissue conditions. Figure 2 pools data from all samples; all qMRI parameters were higher in WM than GM ROIs. MWF results were comparable across tissue conditions, but ANOVA detected higher MTR, qMT-F, and short T_1-F values in thawed/fixed tissue compared to fresh. Figure 3 pools data from samples scanned fresh/thawed and fresh/fixed separately and plots qMRI parameters vs. LFB to demonstrate correlations. For some plots MTR and qMT-F correlated with LFB within WM ROIs. Figure 4 shows correlations among each pair of qMRI parameters, with consistent results across tissue conditions. Figure 5 shows two representative human samples from the posterior/frontal periventricular WM and their parameter maps. ROI data pooled from all human samples show differences among values in normal appearing WM (NAWM), WM lesions, and GM ROIs.

Discussion

We expected MTR and qMT-F to be higher for fixed tissue than fresh based on previous literature[2], which explains this increase as tissue fixation causing expansion of the spaces between layers of the myelin sheath, which may cause more exchange between the macromolecular and water pools and increase qMT-F. We have found similar results for thawed tissue, so we conjecture that freezing it may also have expanded the space between the myelin. The outlier pixels in the MWF maps are from using a constant T_2 cutoff, as a few voxels had peaks inconsistent with this cutoff. The outliers and lower R^2 values in Figure 4 for plots with short T_1-F may be due to inexact ROI correspondence from imperfect EPI data unwarping/registration. The histology slices are not exactly the same as the MR slices, as seen in Figure 1, which also affects ROI correspondence. The LFB insets in Figure 1f show intact cells after both the freezing/thawing and fixation processes. However, the duration of freezing was a couple weeks, so the long-term effects of tissue freezing are unknown and could be studied in the future.

Conclusion

Thawed tissue MR parameters had modest increases compared to fresh, and the samples maintained cell integrity. As a result, tissue freezing is a reasonable alternative tissue preservation method to fixation, and maintains the ability to conduct immunohistochemistry.

Acknowledgements

This work is supported by NIH grant P30AG072931-03S1. We thank the myelin water imaging group at the University of British Columbia for helpful discussions.

References

1. Laule, C., Kozlowski, P., Leung, E., Li, D. K., MacKay, A. L., & Moore, G. W. (2008). Myelin water imaging of multiple sclerosis at 7 T: correlations with histopathology. Neuroimage, 40(4), 1575-1580.

2. Seifert, A. C., Umphlett, M., Hefti, M., Fowkes, M., & Xu, J. (2019). Formalin tissue fixation biases myelin-sensitive MRI. Magnetic resonance in medicine, 82(4), 1504-1517.

3. Shabihkhani, M., Lucey, G. M., Wei, B., Mareninov, S., Lou, J. J., Vinters, H. V., ... & Yong, W. H. (2014). The procurement, storage, and quality assurance of frozen blood and tissue biospecimens in pathology, biorepository, and biobank settings. Clinical biochemistry, 47(4-5), 258-266.

4. Rosene, D. L., & Rhodes, K. J. (1990). Cryoprotection and freezing methods to control ice crystal artifact in frozen sections of fixed and unfixed brain tissue. In Methods in Neurosciences (Vol. 3, pp. 360-385). Academic Press.

5. Murguia, A., Swanson, S. D., Scheven, U., Nielsen, J. F., Fessler, J. A., & Seraji-Bozorgzad, N. Characterizing Tissue Relaxation and Magnetization Transfer in Fresh, Thawed, and Fixed White Matter Tissue Samples. In Proceedings of the 32nd Annual Meeting of the ISMRM. May 2024. Singapore.

6. Whittall, K. P., & MacKay, A. L. (1989). Quantitative interpretation of NMR relaxation data. Journal of Magnetic Resonance (1969), 84(1), 134-152.

7. Sled, J. G., & Pike, G. B. (2001). Quantitative imaging of magnetization transfer exchange and relaxation properties in vivo using MRI. Magnetic Resonance in Medicine: An Official Journal of the International Society for Magnetic Resonance in Medicine, 46(5), 923-931.

8. Henkelman, R. M., Huang, X., Xiang, Q. S., Stanisz, G. J., Swanson, S. D., & Bronskill, M. J. (1993). Quantitative interpretation of magnetization transfer. Magnetic resonance in medicine, 29(6), 759-766.

9. Wang, Y., van Gelderen, P., de Zwart, J. A., & Duyn, J. H. (2020). B0-field dependence of MRI T1 relaxation in human brain. NeuroImage, 213, 116700.

10. Jezzard, P., & Balaban, R. S. (1995). Correction for geometric distortion in echo planar images from B0 field variations. Magnetic resonance in medicine, 34(1), 65-73.

11. Stanisz, G. J., Odrobina, E. E., Pun, J., Escaravage, M., Graham, S. J., Bronskill, M. J., & Henkelman, R. M. (2005). T1, T2 relaxation and magnetization transfer in tissue at 3T. Magnetic Resonance in Medicine: An Official Journal of the International Society for Magnetic Resonance in Medicine, 54(3), 507-512.

Figures

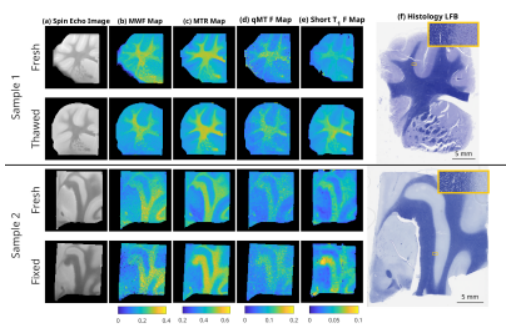

Fig 1. qMRI maps and LFB histology stains for two representative sheep brain samples at the globus pallidus level. Sample 1 (rows 1-2, coronal slice) was scanned fresh and thawed, and Sample 2 (rows 3-4, sagittal slice) was scanned fresh and fixed. (a) Spin echo images. (b) MWF maps calculated with 20 ms T_2 cutoff. (c) MTR maps from MT contrast images at average of -10kHz/10kHz off-resonance. (d) qMT solid pool fraction maps. (e) Short T_1 fraction maps. (f) LFB OD histology; insets show zoomed-in views with individual cells.

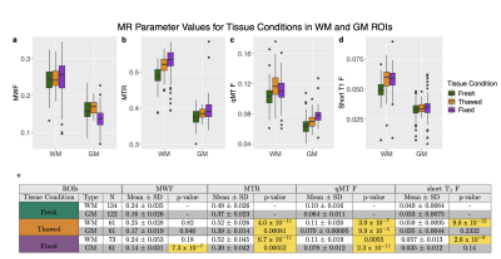

ROIs			MWF		MTR		qMT F		short T_1 F	
Tissue Condition	Type	N	Mean ± SD	p-value	Mean ± SD	p-value	Mean ± SD	p-value	Mean ± SD	p-value
Fresh	WM	134	0.34 ± 0.025	-	0.49 ± 0.026	-	0.10 ± 0.016	-	0.048 ± 0.0084	-
	GM	122	0.36 ± 0.026	-	0.37 ± 0.023	-	0.064 ± 0.011	-	0.033 ± 0.0075	-
Thawed	WM	61	0.35 ± 0.028	0.02	0.52 ± 0.028	4.0×10^{-11}	0.11 ± 0.020	3.9×10^{-3}	0.049 ± 0.0095	9.8×10^{-10}
	GM	61	0.37 ± 0.019	0.040	0.39 ± 0.014	0.00391	0.075 ± 0.00905	9.9×10^{-5}	0.035 ± 0.0044	0.2332
Fixed	WM	73	0.34 ± 0.053	0.18	0.52 ± 0.045	6.7×10^{-11}	0.11 ± 0.019	0.0055	0.057 ± 0.013	2.6×10^{-6}
	GM	61	0.34 ± 0.031	7.3×10^{-7}	0.39 ± 0.042	0.00152	0.078 ± 0.0112	2.3×10^{-11}	0.035 ± 0.013	0.14

Fig 2. (a-d) Box plots (interquartile range, whiskers: 1.5-times interquartile range, outliers as dots) of mean-adjusted qMRI parameter values (across individual samples) for all sheep samples. (e) Chart with mean +/- standard deviation and p-values from Mann–Whitney U testing of thawed parameters compared to fresh and fixed parameters compared to fresh. Yellow cells mark statistically significant p-values. For MTR and qMT-F, both thawed and fixed means are statistically significantly different from fresh. MWF, MTR, and qMT-F values are consistent with literature[1-2,11].

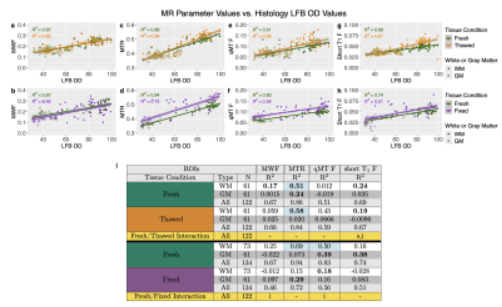

ROIs			MWF	MTR	qMT F	short T_1 F
Tissue Condition	Type	N	R^2	R^2	R^2	R^2
Fresh	WM	61	**0.17**	**0.51**	0.012	**0.24**
	GM	61	0.0018	**0.24**	-0.019	0.035
	All	122	0.07	0.06	0.31	0.69
Thawed	WM	61	0.089	**0.58**	0.45	**0.19**
	GM	61	0.025	0.030	0.0068	-0.0098
	All	122	0.06	0.04	0.59	0.67
Fresh, Thawed Interaction	All	122	-	-	-	s,i
Fresh	WM	73	-0.25	0.69	0.30	0.14
	GM	61	-0.022	0.073	**0.30**	**0.38**
	All	134	0.07	0.04	0.83	0.74
Fixed	WM	73	-0.012	0.15	**0.18**	-0.026
	GM	61	0.097	**0.29**	0.16	-0.043
	All	134	0.46	0.72	0.56	0.51
Fresh, Fixed Interaction	All	122	i	-	i	-

Fig 3. (a-h) Correlation between qMRI/LFB mean-adjusted values for fresh/thawed (row 1), and fresh/fixed (row 2) sheep data. Fresh data have been separated into 2 groups as each scan pair for 1 sample corresponds to 1 LFB image. (i) Chart with R^2 across all ROIs and WM/GM ROIs, bold for p<0.01. All conditions show correlation with LFB for all ROIs. Blue cells show R^2 values ≥ 50 for WM ROIs. Yellow rows show GLM interaction term between tissue condition/LFB; s: statistically different slopes, i: statistically different intercepts, indicating differential correlation based on condition.

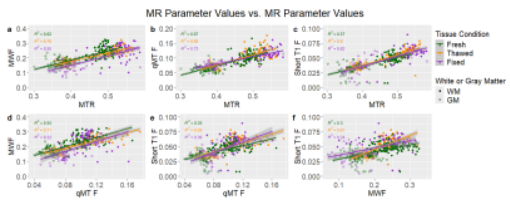

Fig 4. Correlation among qMRI parameter mean-adjusted values for sheep data. MTR and qMT-F are most strongly correlated, likely since they were both derived from the same MT data (b). MWF and short T_1-F also correlate well with MTR for all conditions (a,c). Unlike histology images, where image coregistration is more difficult, the same ROIs were used for all qMRI maps here. Fits are similar among tissue conditions for all pairs of parameters, further suggesting that thawed samples are a viable option for qMRI analysis compared to fresh/fixed samples.

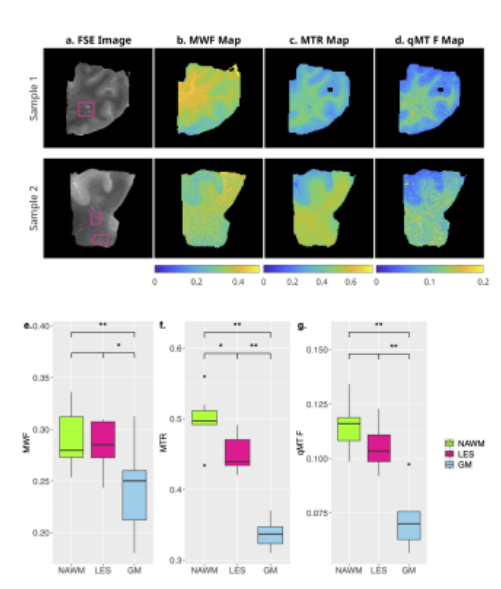

Fig 5. Human tissue preliminary data in 2 different samples with same protocol[5] except with 1mm slice thickness/1mm slice gap. (a) Fast spin echo (FSE) images (TR=4000 ms, TE_{eff}=40 ms, ESP=10 ms, segments/ETL=32/8, matrix size=256x256) with example lesion ROIs outlined in pink. (b-d) qMRI maps. Dark spots in c-d are from signal void in that region. (e-g) Box plots of mean-adjusted MR parameters for 7 samples in 12 NAWM, 10 lesion (LES), and 8 GM ROIS. Statistically significant Mann–Whitney U results are marked with *(p<0.05), **(p< 0.01). Lesion ROIs exhibited lower MTR values than NAWM.